Electronic Supplementary Material (ESI) for Journal of Materials Chemistry A.

Supplementary Information

Highly Flexible and Sensitive Temperature Sensors based on $Ti_3C_2T_x$ (MXene) for Electronic Skin

Zherui Cao,†[ab] Yina Yang,†[ab] Yinghui Zheng,[c] Wei Wu,[d] Fangfang Xu,[a] Ranran Wang,*[a] and Jing Sun[a]

a. State Key Laboratory of High Performance Ceramics and Super fine Microstructure, Shanghai Institute of Ceramics, Chinese Academy of Sciences, 1295 Ding Xi Road, Shanghai 200050, P. R. China.

E-mail: wangranran@mail.sic.ac.cn

b. University of Chinese Academy of Sciences, 19 Yuquan Road, Beijing 100049, P. R. China.

c. State Key Laboratory of High Field Laser Physics, Shanghai Institute of Optics and Fine Mechanics, Chinese Academy of Sciences, Shanghai 201800, China.

d. Thermo Fisher Scientific

† These authors contributed equally to this work.

Movie S1. The surface morphologies change of the TMA-$Ti_3C_2T_x$ based sensor during heating process.

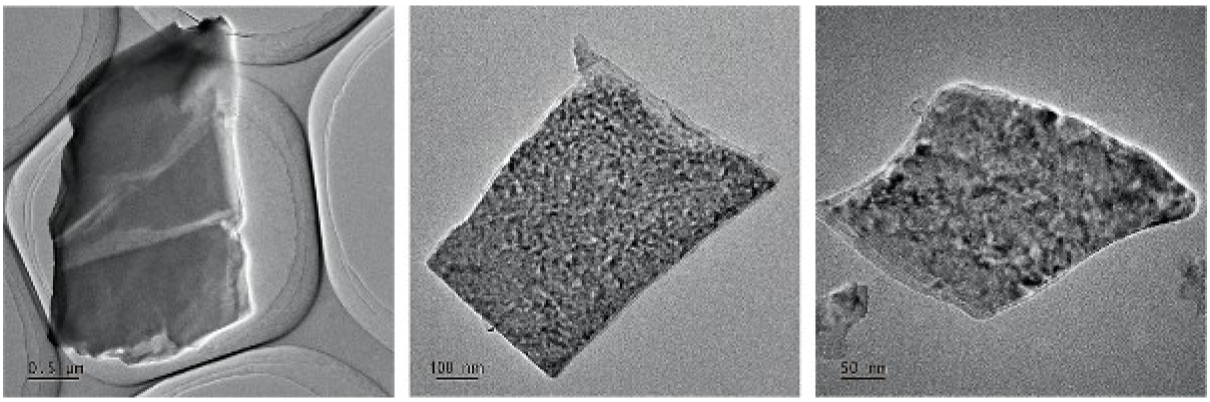

Figure S1. TEM images of TMA-$Ti_3C_2T_x$ (a), HF6-d3-$Ti_3C_2T_x$ (b), and HF18-d2-$Ti_3C_2T_x$ (c).

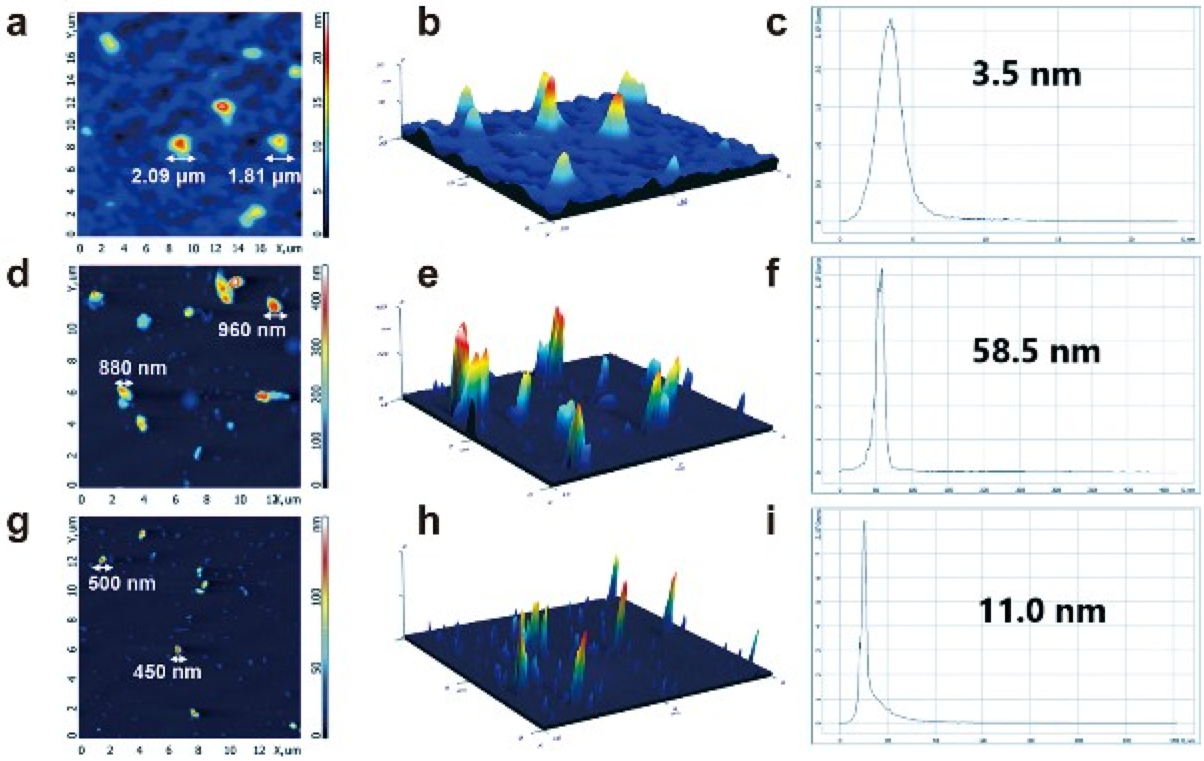

Figure S2. AFM results of TMA-$Ti_3C_2T_x$ (a-c), HF6-d3-$Ti_3C_2T_x$ (d-f), and HF18-d2-$Ti_3C_2T_x$ (g-i).

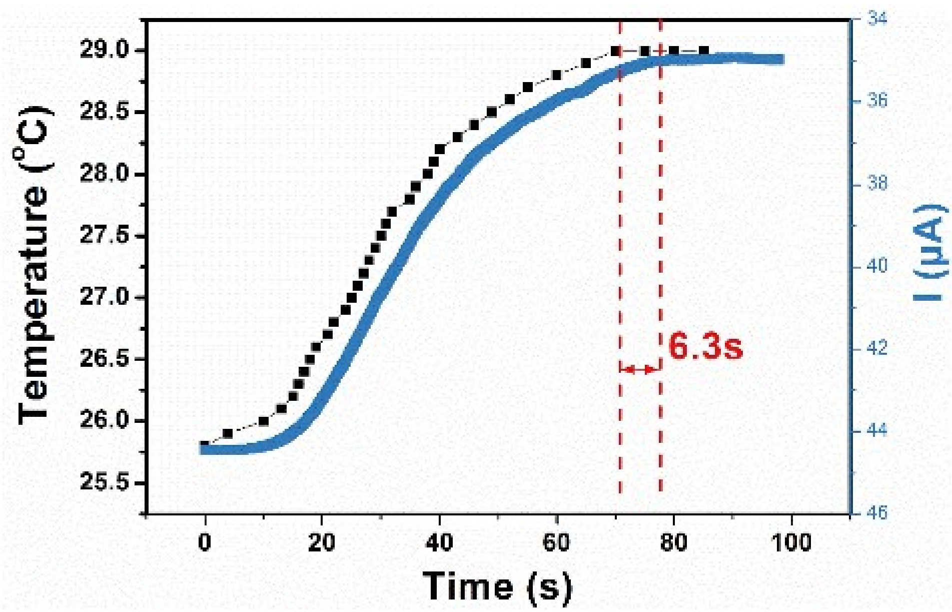

Figure S3. The response time curves of the $Ti_3C_2T_x$ based sensor under increasing temperature.

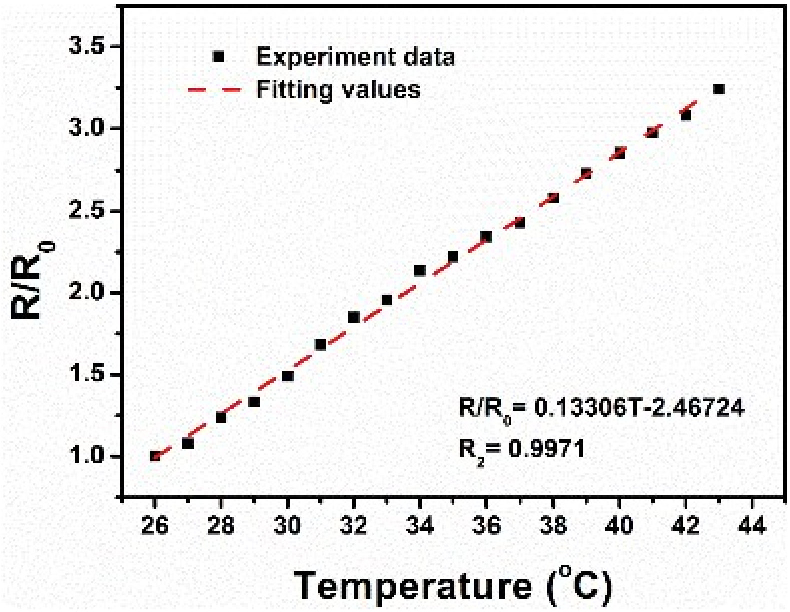

Figure S4. Resistance variations versus temperature of the $Ti_3C_2T_x$ based sensor during the first cycle.

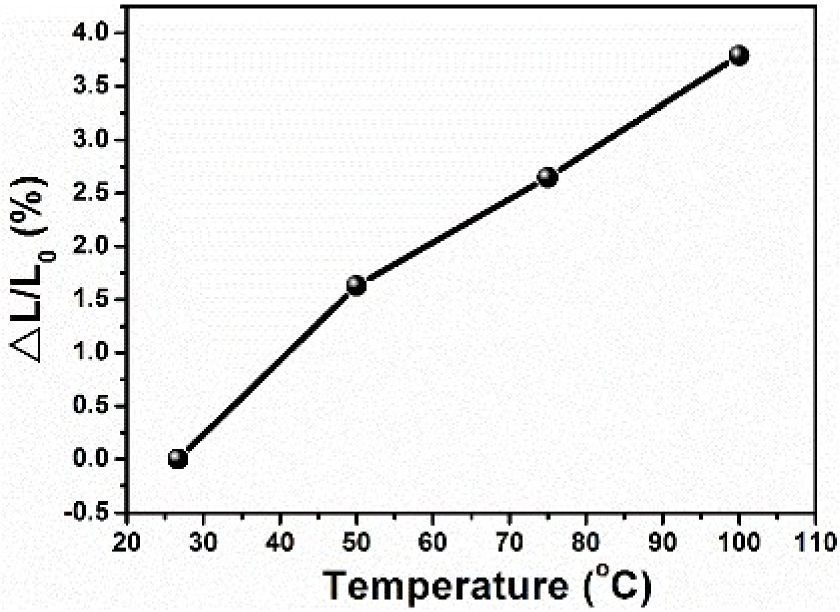

Figure S5. Length variations versus temperature of a PDMS block (25×5×5 mm^3).

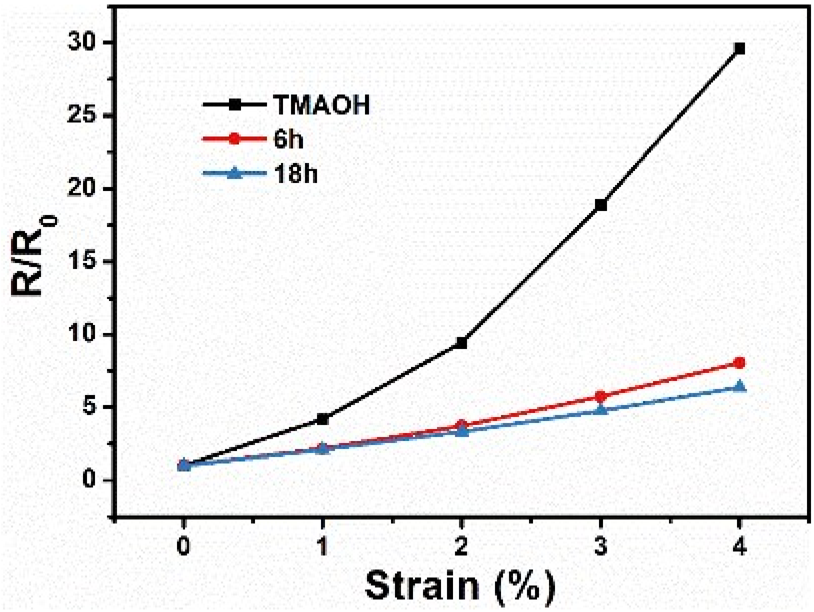

Figure S6. Resistance variations versus strain of the three kinds of $Ti_3C_2T_x$ based sensors.

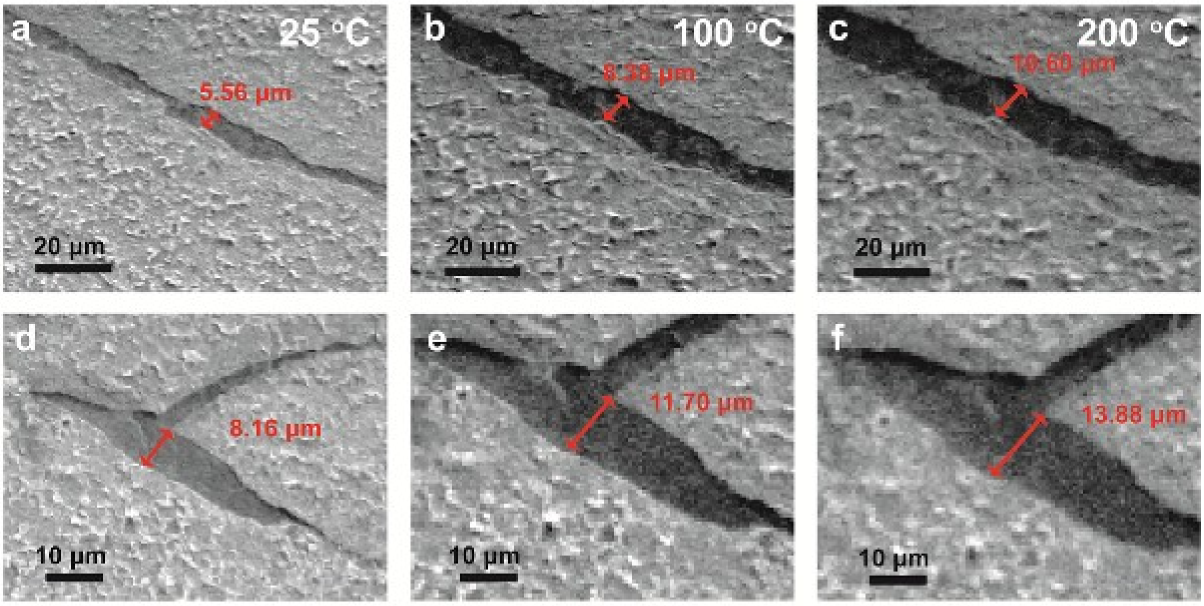

Figure S7. The microstructure variation of the cracks of the TMA-$Ti_3C_2T_x$ film at the temperature of 25, 100, and 200 °C.

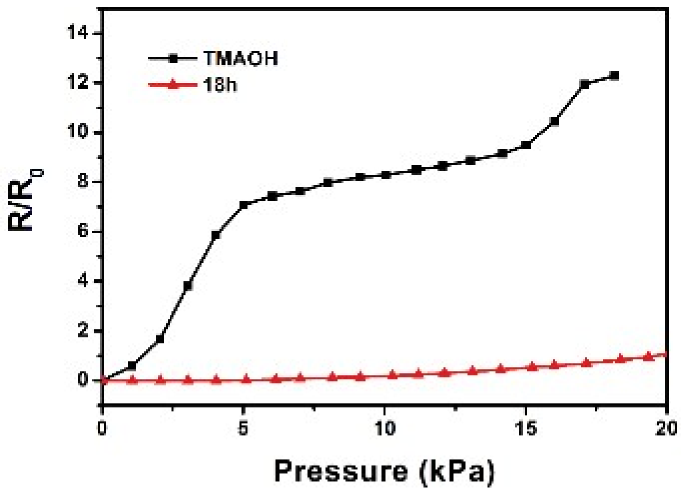

Figure S8. Resistance variation versus pressure of the $Ti_3C_2T_x$ based sensors.

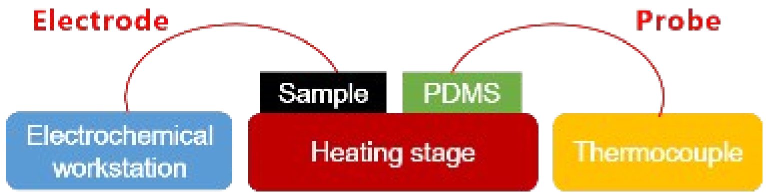

Figure S9. Schematic illustration of the test method for the temperature sensing performance.

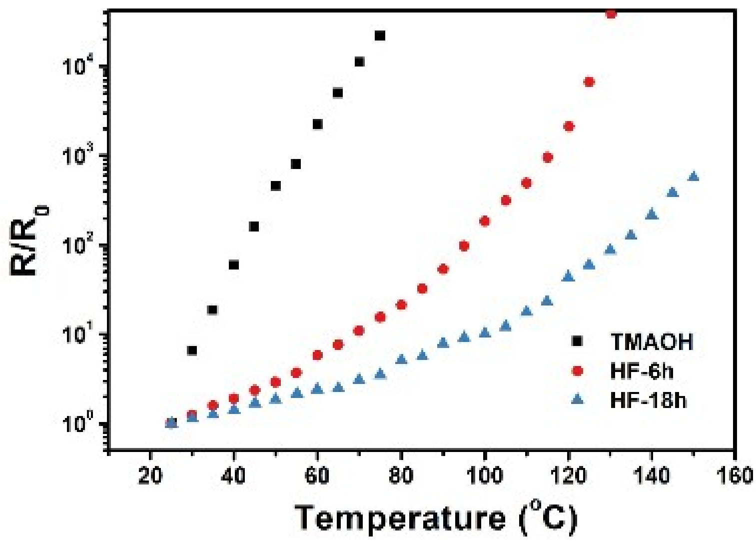

Figure S10. Resistance variation versus temperature of the three kinds of $Ti_3C_2T_x$ based sensors measured by an infrared imaging device.

Table S1. The Comparison of the typical sensing properties of the previously reported studies.

Materials	Sensitivity	Range (°C)	Time	Accuracy (°C)	Flexible
GNWs/PDMS[1]	0.214 $°C^{-1}$	35–45	1.6 s	0.1	○
Ni microparticle-filled PE/PEO binary polymer composite[2]	0.10–0.90 $°C^{-1}$	20-45		±2.7	○
Graphite powders in PDMS[3]	0.286 $°C^{-1}$	30–110			○
rGO/PU[4]	0.0134 $°C^{-1}$	30-80		0.2	○
Cr /Au/PU[5]	0.002778 $°C^{-1}$	22–45			○
Pt/PI[6]	0.00219 $°C^{-1}$	20–60	<80 ms	2	○
AuNP/PU[7]	0.41 M Ω $°C^{-1}$	10–42		0.1	○
FET with rGO/PVDF-TrFE channel[8]	0.0136 $°C^{-1}$	30–80		0.1	○
Polyaniline nanofiber with CNT TFT[9]	0.01 $°C^{-1}$	15–45	1.8 s		○
rGO[10]	0.0055 $°C^{-1}$	0–100			○
CNT-PEDOT:PSS[11]	0.0025 $°C^{-1}$	21–80	<1 s		○
CNT-PEDOT:PSS[12]	0.0061 $°C^{-1}$	22–48			○
CuNW mesh/PI[13]	0.7 Ω $°C^{-1}$	RT–48			○
ZnO NW/PU fiber[14]	0.00393 $°C^{-1}$	25–50			○
graphene nanoplatelets (GNPs)/ silicone rubber[15]	0.0371 $°C^{-1}$	10-60	5 s		○
Graphene/PI[16]	-0.0148 $°C^{-1}$	20-180			○
PEI/rGO[17]	0.013 $°C^{-1}$	25-45	0.654 s	0.1	○
Ligand-Treated Ag Nanocrystal /PDMS[18]	0.5 $°C^{-1}$	30-50	15 s		○
MWCNTs/Si[19]	-8×10^{-8} $°C^{-1}$	25-190			X
CNT-Si/Glass[20]	-0.0072 $°C^{-1}$	23–82			X
MWCNTs -GMSA/Glass[21]	-0.0054 $°C^{-1}$	24–86			X
MWCNTs[22]	-0.001 $°C^{-1}$	-268.8-147			X
$Ti_3C_2T_x$ /PDMS (Our work)	0.03-986 $°C^{-1}$	20-140	6.3 s	0.1	○

References

1. J. Yang, D. Wei, L. Tang, X. Song, W. Luo, J. Chu, T. Gao, H. Shi and C. Du, *RSC Adv.*, 2015, **5**, 25609-25615.

2. J. Jeon, H. B. Lee and Z. Bao, *Adv. Mater.*, 2013, **25**, 850-855.

3. W. P. Shih, L. C. Tsao, C. W. Lee, M. Y. Cheng, C. Chang, Y. J. Yang and K. C. Fan, *Sensors*, 2010, **10**, 3597-3610.

4. T. Q. Trung, S. Ramasundaram, B. U. Hwang and N. E. Lee, *Adv. Mater.*, 2016, **28**, 502-509.

5. Y. Chen, B. Lu, Y. Chen and X. Feng, *Sci. Rep.*, 2015, **5**, 11505.

6. M. D. Dankoco, G. Y. Tesfay, E. Benevent and M. Bendahan, *Mater. Sci. Eng., B*, 2016, **205**, 1-5.

7. T. P. Huynh and H. Haick, *Adv. Mater.*, 2016, **28**, 138-143.

8. T. Q. Trung, S. Ramasundaram, S. W. Hong and N.-E. Lee, *Adv. Funct. Mater.*, 2014, **24**, 3438-3445.

9. S. Y. Hong, Y. H. Lee, H. Park, S. W. Jin, Y. R. Jeong, J. Yun, I. You, G. Zi and J. S. Ha, *Adv. Mater.*, 2016, **28**, 930-935.

10. D. H. Ho, Q. Sun, S. Y. Kim, J. T. Han, D. H. Kim and J. H. Cho, *Adv. Mater.*, 2016, **28**, 2601-2608.

11. S. Harada, Kanao, K., Yamamoto, Y., Arie, T., Akita, S., Takei, K, *ACS Nano*, 2014, **8**, 12851-12857.

12. W. Honda, Harada, S., Arie, T., Akita, S., Takei, K, *Adv. Funct. Mater.*, 2014, **24**, 3299-3304.

13. S. Han, M. K. Kim, B. Wang, D. S. Wie, S. Wang and C. H. Lee, *Adv. Mater.*, 2016, **28**, 10257-10265.

14. X. Liao, Q. Liao, Z. Zhang, X. Yan, Q. Liang, Q. Wang, M. Li and Y. Zhang, *Adv. Funct. Mater.*, 2016, **26**, 3074-3081.

15. M. H. Tian, Ying; Wang, Weihua; Li, Ruiqi; Liu, Ping; Liu, *J. Mater. Res.*, 2014, **29**, 1288-1294.

16. D. Kong, L. T. Le, Y. Li, J. L. Zunino and W. Lee, *Langmuir*, 2012, **28**, 13467-13472.

17. Q. Liu, H. Tai, Z. Yuan, Y. Zhou, Y. Su and Y. Jiang, *Advanced Materials Technologies*, 2019, **4**, 1800594.

18. J. Bang, W. S. Lee, B. Park, H. Joh, H. K. Woo, S. Jeon, J. Ahn, C. Jeong, T. i. Kim and S. J. Oh, *Adv. Funct. Mater.*, 2019, DOI: 10.1002/adfm.201903047, 1903047.

19. S. Vollebregt, F. D. Tichelaar, H. Schellevis, C. I. M. Beenakker and R. Ishihara, *Carbon*, 2014, **71**, 249-256.

20. M. T. S. A. Chani, A.M.; Karimov, K.S.; Bashir, M.; Khan, S.B.; Rahman, M.M, *International Journal of Electrochemical Science*, 2015, **10**, 3784-3791.

21. K. S. Karimov, M. Abid, M. Saleem, K. M. Akhmedov, M. M. Bashir, U. Shafique and M. M. Ali, *Physica B: Condensed Matter*, 2014, **446**, 39-42.

22. A. Di Bartolomeo, M. Sarno, F. Giubileo, C. Altavilla, L. Iemmo, S. Piano, F. Bobba, M. Longobardi, A. Scarfato, D. Sannino, A. M. Cucolo and P. Ciambelli, *Journal of Applied Physics*, 2009, **105**, 064518.